

Chemical Science

rsc.li/chemical-science



ISSN 2041-6539

Cite this: *Chem. Sci.*, 2020, **11**, 9067

All publication charges for this article have been paid for by the Royal Society of Chemistry

Received 19th June 2020
Accepted 8th August 2020

DOI: 10.1039/d0sc03437a
rsc.li/chemical-science

Introduction

Complex biochemical systems, in which weak intra- and intermolecular interactions between covalent-bound macromolecules provide both rigidity and an extensive dynamic behaviour, inspire modern coordination chemistry to design discrete and extended supramolecular architectures *via* metal-directed metal-ligand self-assembly.¹ An impressive example of mimicking enzymes was demonstrated in the group of C. A. Mirkin using so called weak-link approach.^{1e,f} To this effect, Lewis-acidic metal-based coordination centres together with appropriate building blocks are needed that are able to design supramolecular assemblies.^{1g,h} In addition to widely used E-donor ligands (E = N, O, S, *etc.*), polyphosphorus ligand complexes proved to be able to coordinate metal cations by P centres and to give, at certain conditions, supramolecular assemblies of spherical architectures possessing fullerene² or non-fullerene³ topology. However, most of these spherical supramolecules are obtained for pentaphosphaphaferrocenes,⁴ whereas a range of end-deck *cyclo-P₄* complexes remain unexplored in this context.⁵ Only three types of supramolecules based on the $\{\text{Cp}^{\text{R}}\text{Ta}(\text{CO})_2(\eta^4\text{-P}_4)\}$ complexes ($\text{Cp}^{\text{R}} = 1,3\text{-C}_5\text{H}_3t\text{Bu}_2$ (Cp^{R} , **1a**),^{5a} $\text{Cp}^{\text{R}} = 1,2,4\text{-C}_5\text{H}_2t\text{Bu}_3$ (Cp^{R} , **1b**)) are

known so far.⁶ The first type is represented by a family of $[\{\text{Cp}^{\text{R}}\text{Ta}(\text{CO})_2(\eta^4\text{-P}_4)\}_6\{\text{CuX}\}_8]$ supramolecules (**2**: $\text{Cp}^{\text{R}} = \text{Cp}^{\text{R}}$, $\text{Cp}^{\text{R}}\text{Cl}$, $\text{Cp}^{\text{R}}\text{Br}$) in which the inorganic scaffold has a non-classical fullerene topology being composed exclusively of $\{\text{cyclo-P}_4\}$ four- and $\{\text{Cu}_2\text{P}_4\}$ six-membered rings. Two other types of spheres demonstrate unmatched 'peanut'-like [**1a**₁₀{CuI}₁₄] (**3**) and 'pear'-like [**1a**₅{CuI}₁₂(CH₃CN)₅] (**4**) scaffolds.^{6b} Unlike many supramolecules based on *cyclo-P₅* building blocks, none of these four-membered ring-based spheres feature guest inclusions or even possess a guest accessible void.

A way to realize host-guest chemistry is to use a larger Lewis-acidic metal cation free of any additional ligand occupying a coordination site. Moreover, the introduction of a fourth reaction component stimulating the degree of freedom in a self-organising process might create an extra chance of host-guest ability. Such a fourth component could be a linker that enables flexible aggregation. Herein we report on the self-assembly reaction of P₄Se₃, $\{\text{Cp}^{\text{R}}\text{Ta}(\text{CO})_2(\eta^4\text{-P}_4)\}$ (**1a**), AgSbF₆ and the flexible dinitrile NC(CH₂)₇CN to give a 2D coordination network in which a barrel-like supramolecular host-guest P₃Se₄@ $[(\{\text{Cp}^{\text{R}}\text{Ta}(\text{CO})_2(\eta^4\text{-P}_4)\}\text{Ag})_8]^{8+}$ assemblies of 2.49 nm in size are connected by dinitrile linkers.

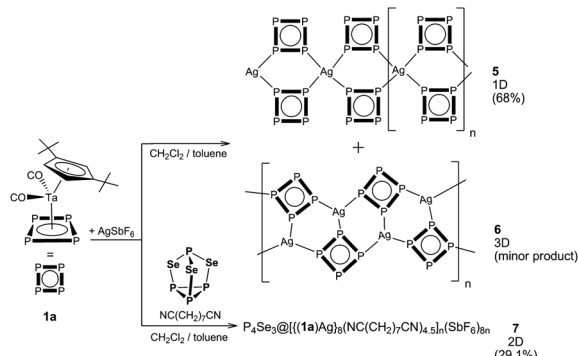
Results and discussion

To approach the task of host-guest chemistry starting with a four-membered building block, the two-component self-assembly of **1a** and AgSbF₆ was studied beforehand. A

Institute of Inorganic Chemistry, University of Regensburg, 93040 Regensburg, Germany. E-mail: Manfred.Scheer@ur.de

† Electronic supplementary information (ESI) available: Details on X-ray structural and spectroscopic characterization. CCDC 2009904–2009906. For ESI and crystallographic data in CIF or other electronic format see DOI: [10.1039/d0sc03437a](https://doi.org/10.1039/d0sc03437a)



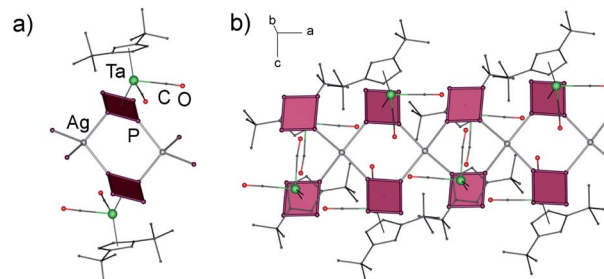
Fig. 1 Reaction of **1** with AgSbF_6 , P_4Se_3 and $\text{NC}(\text{CH}_2)_7\text{CN}$.

colourless solution of AgSbF_6 in CH_2Cl_2 was layered with a yellow solution of **1a** in toluene with a CH_2Cl_2 : toluene middle-layer (2 : 1). During the diffusion process, two different crystalline phases are formed (Fig. 1): orange plates of **5** and a few orange octahedra of **6**. Unfortunately, the change of neither the stoichiometry nor the concentration of the starting materials nor the layering of the reaction solution after a complete diffusion with hexane, pentane or Et_2O led to a selective formation of one of the products.

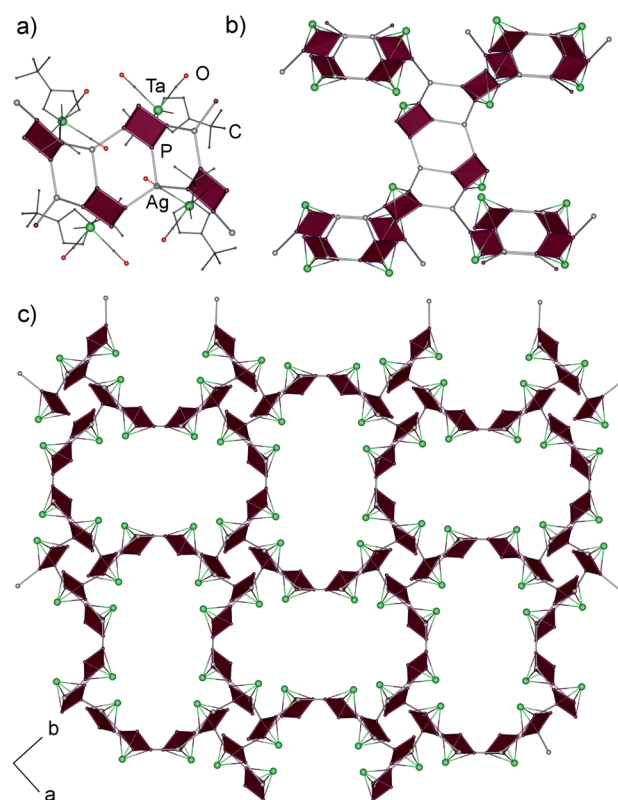
According to X-ray diffraction studies, the main product of the reaction of **1a** with AgSbF_6 is a 1D coordination polymer $[(\text{Cp''Ta}(\text{CO})_2(\mu_3, \eta^4:\eta^1:\eta^1-\text{P}_4)_2\text{Ag})_n(\text{SbF}_6)_n$ (**5**) consisting of chains with $\{\text{Ag}(\mathbf{1a})_2\}$ repeating units (Fig. 2a).[‡] The Ag ions show a distorted tetrahedral coordination by four P atoms of four different *cyclo-P₄* ligands ($\text{P}-\text{Ag}-\text{P}$ 90.3–140.5°), which, in turn, coordinate to another $\{\text{Ag}_2\text{P}_4\}$ moiety in a 1,2-fashion (Fig. 2b). This structural motif, $\{\text{M}_2\text{P}_4\}$, has been known for other supramolecular aggregates based on polyphosphorus complexes and $\text{M}(\text{i}) = \text{Cu}$,^{2,6a,7} Ag ,⁸ but has not been found for the *cyclo-P₄* derivatives. The P–P bond lengths vary in a range between 2.149(5) and 2.179(5) Å and are in agreement with those in the free complex **1a** (2.150(2)–2.173(3) Å),^{5a} whereas the Ag–P bond lengths range between 2.494(3) and 2.563(3) Å. The SbF_6^- counter anions and the CH_2Cl_2 solvent molecules separate the chains.

Product **5** is insoluble in *n*-pentane and *n*-hexane, sparingly soluble in CH_2Cl_2 and fragmentises in N-donor solvents such as pyridine and CH_3CN . In the ESI-MS spectrum, fragments containing **1a**, Ag^+ and SbF_6^- are visible, with the highest peak at $m/z = 2604.7$, which can be assigned to $[\{\mathbf{1a}\}_4\text{Ag}_2\text{SbF}_6]^+$. The ^1H and ^{31}P NMR spectra of **5** in CD_3CN show signals corresponding to free **1a** that corroborates with the expected fragmentation of **5** in CD_3CN .

Interestingly, the other coordination polymer $[(\text{Cp''Ta}(\text{CO})_2(\mu_4, \eta^4:\eta^1:\eta^1-\text{P}_4)_2\text{Ag})_n(\text{SbF}_6)_n$ (**6**) was formed as a minor byproduct in the same reaction. This solvent-free phase, crystallized as orange octahedra, proved to have the same 2 : 1 ratio of **1a** : AgSbF_6 as **5** and therefore represented a structural isomer of **5** which precluded a selective isolation and characterisation of the individual compounds by applying the appropriate stoichiometry of the educts. In contrast to **5**, single crystal X-ray structure analysis of **6** revealed a 3D

Fig. 2 (a) Repeating unit and (b) section of 1D coordination polymer in **5**. Counter anions SbF_6^- are omitted for clarity.

coordination polymer crystallizing as a racemic conglomerate in the chiral space groups $P4_12_12$ or $P4_32_12$.[‡] In the 3D framework all *cyclo-P₄* ligands coordinate to Ag^+ cations in a 1,2,3-coordination mode (Fig. 3), occurring only once in the peanut-like supramolecule.^{6b} The tetrameric repeating $\{(\mathbf{1a})_4\text{Ag}_4\}$ units in **6** are constructed by the edge-sharing of three six-membered rings of $\{\text{Ag}_2\text{P}_4\}$.^{8a} The tetramers possess a curved shape due to a distorted triangular coordination environment of Ag (the $\text{P}-\text{Ag}-\text{P}$ angles are in the range of 103.4–130.5°, Fig. 3a). Each unit is joined to four other neighbouring units (Fig. 3b) *via* one Ag–P coordinative bond to form a chiral 3D diamond-like network (**dia⁹**) with expanded channels (Fig. 3c). Despite being large (1.2–1.3 nm[§]), these channels do not provide accessible voids

Fig. 3 (a) Repeating unit of **6** surrounded by four similar units (b) and (c) a section of the 3D coordination polymer in **6**. Cp'' and carbonyl ligands as well as counter anions SbF_6^- are omitted for clarity.

and are occupied by Cp'' and CO ligands of **1a** as well as by SbF_6^- anions. The P–P bonds lengths range from 2.146(3) to 2.180(4) Å, being in agreement with the bond lengths in **5** and **1a**,^{5a} whereas the Ag–P bond lengths vary in a range between 2.446(3) and 2.493(3) Å.

Interestingly, the curved tetrameric repeating unit in the structure of **6** can potentially be extended to some kind of a cylindrical core similar to previously reported non-classical fullerene-like cores **2**.⁶ However, in **6** the $\{\text{Cp}''\text{Ta}(\text{CO})_2\}$ units point out alternatively on the different sides of the *cyclo-P₄* ligands of the concave tetramer. While in any possible cylindrical core all $\{\text{Cp}''\text{Ta}(\text{CO})_2\}$ units should point outside.

To overcome this difficulty and to direct the self-assembly process to the formation of a convex shell based on Ag cations and complexes **1a**, we used a cage molecule P_4Se_3 as a rather small template. Moreover, to induce coordinative freedom and flexibility to form potential host–guest cages, we targeted the introduction of a flexible aliphatic linker as *e.g.* the dinitriles $\text{NC}(\text{CH}_2)_n\text{CN}$ with $n \geq 7$, because they deliver the needed distance to the next possible formed sphere. To interconnect potentially formed supramolecular assemblies of **1a** and AgSbF_6 templated by P_4Se_3 , we used the linker $\text{NC}(\text{CH}_2)_7\text{CN}$ in a four-component self-assembly process.

A colourless solution of AgSbF_6 in CH_2Cl_2 is first layered with a mixture of CH_2Cl_2 and toluene (2 : 1) and then with a yellow solution of **1a**, P_4Se_3 , and $\text{NC}(\text{CH}_2)_7\text{CN}$ in toluene. The intermediate layer of the mixed solvents is used to slow down the diffusion and thus facilitate the growth of crystals better suitable for X-ray structure analysis. The AgSbF_6 , **1a**, P_4Se_3 and $\text{NC}(\text{CH}_2)_7\text{CN}$ were taken in a ratio of 1 : 1 : 1.5 : 10; the 10-fold excess of the dinitrile is required to avoid the formation of the

insoluble polymers **5** and **6**. By doing this, orange prismatic crystals of **7** in 29% yield were formed (Fig. 1). Variation of the stoichiometry only leads to the occurrence of by-products and the formation of **7** in lower yields.

Single crystal X-ray structure analysis revealed the formation of a 2D polymeric network of interconnected supramolecular aggregates of $\text{P}_4\text{Se}_3@[(\text{Cp}''\text{Ta}(\text{CO})_2(\text{n}^4\text{-P}_4))\text{Ag}]_8(\text{NC}(\text{CH}_2)_7\text{CN})_{4.5}]_n(\text{SbF}_6)_{8n}$ (**7**) (Fig. 4). In this square lattice coordination network the nodes represent novel self-assembled aggregates $[(\text{1a})\text{Ag}]_8^{8+}$ of 2.49 nm in size (Fig. 4a, see ESI† for details).¶ In the inorganic core of the nodes, eight *cyclo-P₄* units and eight Ag ions are assembled in a square-antiprismatic arrangement of eight joined six-membered $\{\text{Ag}_2\text{P}_4\}$ rings (Fig. 4b). This 40-vertex arrangement closely resembles two fused tetrameric units of **6**; every *cyclo-P₄* ligand (P–P: 2.131(5)–2.177(5) Å) coordinates to three Ag cations, again in a 1,2,3-mode. However, the Ag environment is tetrahedral, as every silver cation, in addition to three P atoms of three **1a** units, is also coordinated by one dinitrile linker (2.179(17) to 2.305(14) Å). The Ag–P bond lengths vary from 2.477(3) to 2.528 (3) Å. The similarity of the inorganic cores in **6** and **7** is underlined by P–Ag–P angles that vary from 97.3(1) to 127.4(1)° being similar to those in **6** despite the difference in the coordination number of Ag.

These supramolecular assemblies represent the first doughnut-like *cyclo-P_n*-based structure open at two sides. Cyclic or cylindrical molecules are rather abundant in different classes of coordination compounds. Among them, the closest analogues of cylindrical ligand-based supramolecules usually do not act as molecular containers.¹⁰ A doughnut-shaped Ti-oxo clusters with a permanent MOF-like porosity and high CO_2 adsorption capacity was recently reported.¹¹ Two bowl-like

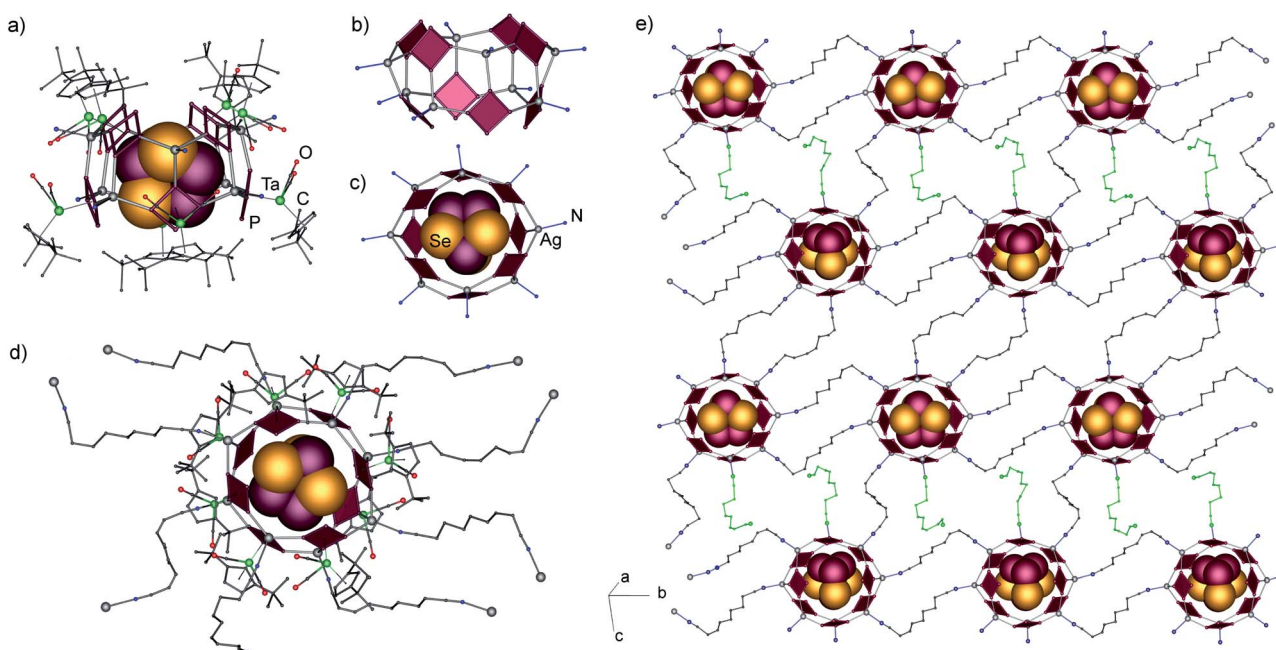


Fig. 4 (a) Supramolecular node, (b) its 40-vertex inorganic core (c) containing a P_4Se_3 guest molecule, (d) node with outgoing linkers, (e) 2D network of interconnected nodes in **7**. The guest is depicted in the space-filling model. Non-coordinating linker units are highlighted in green. $\{\text{Cp}''\text{Ta}(\text{CO})_2\}$ fragments and counter-anions are omitted for clarity.



supramolecules based on pentaphosphaferroocene and Cu(i) halides were just recently obtained in our group, which are open only at one side, $[\{Cp^*Fe(\eta^5-P_5)\}_{11}\{CuX\}_{15-x}]$ ($X = Cl, Br; x = 0.45-1.55$).^{2d} This makes the 'doughnut' in 7 the second example only of the open architectures among all supramolecules based on polyphosphorus *cyclo-P_n* ligands ($n = 4, 5$). Additionally, each supramolecular node contains a P_4Se_3 molecule as a guest (Fig. 4c) in its inner void of 0.60×0.68 nm.¹¹ The guest is disordered over two positions with 80 and 20% probability. The fact that the guest is disordered suggests that there are no significant intermolecular host–guest interactions. The shortest intermolecular contacts amount to $3.54-3.77$ Å for the $P_{host}\cdots Se$ contacts and $3.41-3.65$ Å for the $P_{host}\cdots P_{guest}$ contacts¹¹ (see the ESI† for more details). Nevertheless, the tendency of the self-assembly, without the guest, is towards the coordination polymers 5 or 6, which points to the template-driven formation of the host in 7. Perhaps, the cooperative effect of the weak van der Waals interactions between the P and Se atoms of the guest and the P atoms of the host as well as the effect of a rather spherical shape of the P_4Se_3 molecules enable the formation of the supramolecular host assembly.

Every Ag cation is coordinated by one dinitrile linker, however, only seven dinitriles are linked to another supramolecular node, whereas one is terminal. Three nodes are double-bridged by linkers, while the fourth one is linked by a single dinitrile ligand. The positive charge of the eight Ag(i) cations is balanced by eight SbF_6^- anions which occupy both the interlayer space and the meshes of the network. The presence of a terminal dinitrile possessing a non-coordinated donor cyano group shows the conceptual possibility to expand the structure in the third dimension. The separation of the nodes in the resulting layer, represented by $Ag\cdots Ag$ distances, amounts to $12.44-13.99$ Å. The corresponding $N\cdots N$ distances in the bridging dinitrile ligands vary in the range between 9.24 and 10.31 Å, which demonstrates the shortening of the ligands that possess a folded conformation, as compared to 11.76 Å for the calculated length of the linear linker.¹² This correlation demonstrates that the use of a shorter dinitrile with $n = 6$ (10.73 Å in the linear conformation) might also give similar polymers of host–guest agglomerates for **1a**-based supramolecules.

Crystals of 7 are stable in the mother solution for several weeks. 7 is insoluble in hexane and pentane, sparingly soluble in CH_2Cl_2 and shows fragmentation in CH_3CN and pyridine. In the ESI-MS spectrum of 7, fragments containing **1a**, Ag, $NC(CH_2)_2CN$ and SbF_6^- are observed, with the highest peak at $m/z = 2604.7$, which can be assigned to the same molecular ion $[\{1a\}_4Ag_2SbF_6]^+$ as in the case of 5. Similarly to 5 and 6, in CD_3CN 7 undergoes fragmentation. Therefore, the 1H and ^{31}P NMR spectra show only signals of the starting materials.

Conclusions

The self-assembly of the **1a** complex and the coinage metal salt $AgSbF_6$ was studied, and the possibility of forming host–guest complexes based on *cyclo-P₄* ligands was demonstrated for the first time. Moreover, these host–guest agglomerates can be linked in a coordination network, thus representing new

polymeric matrices in which unprecedented barrel-like silver-polypnictogen-containing supramolecules serve as molecular containers. This finding opens new frontiers in the coordination chemistry of *cyclo-P₄* ligand complexes suggesting the design of new supramolecular architectures and exploring the influence of different coinage metal salts, the template effect of different guests as well as the variation of the nature of the linker and its lengths.

Conflicts of interest

There are no conflicts to declare.

Acknowledgements

This work was supported by the Deutsche Forschungsgemeinschaft within the project Sche 384/44-1. Parts of this research (project I-20180049) were carried out at PETRA III at DESY, a member of the Helmholtz Association (HGF). We thank Dr O. Lorbeer for his assistance regarding the use of the beamline P11.

Notes and references

† X-ray structure analysis: compound **5**: $C_{30.35}H_{42.70}AgCl_{0.70}F_6O_8SbTa_2$, orange plate, $M_r = 1449.64$ g mol⁻¹, triclinic, sp. gr. $\bar{P}1$, $a = 10.4796(5)$, $b = 14.2670(6)$, $c = 17.0118(8)$ Å, $\alpha = 96.742(4)$, $\beta = 90.464(4)$, $\gamma = 101.225(4)$ °, $V = 2476.3(2)$ Å³, $Z = 2$, $T = 90$ K, $R_1 = 0.067$, $wR_2 = 0.182$, GOF = 1.00; compound **6**: $C_{15}H_{21}AgF_6O_2P_4SbTa$, orange octahedron, $M_r = 881.77$ g mol⁻¹, tetragonal, sp. gr. $P4_12_12$, $a = b = 19.22628(9)$, $c = 26.5819(2)$ Å, $V = 9825.98(13)$ Å³, $Z = 16$, $T = 90$ K, $R_1 = 0.030$, $wR_2 = 0.062$, GOF = 0.95, Flack parameter = -0.009(5); compound **7**: $C_{328.5}H_{477}N_{18}O_{32}F_{96}P_{72}Cl_{15}Ag_{16}Sb_{16}Ta_{16}Se_6$, orange prism, $M_r = 16\,818.72$ g mol⁻¹, triclinic, sp. gr. $\bar{P}1$, $a = 17.9549(1)$, $b = 22.5635(2)$, $c = 38.3495(4)$ Å, $\alpha = 81.1581(7)$, $\beta = 78.4160(7)$, $\gamma = 73.7720(7)$ °, $V = 14\,534.6(2)$ Å³, $Z = 2$, $T = 80$ K, $R_1 = 0.0895$, $wR_2 = 0.287$, GOF = 1.09. See ESI for more information.

§ The size of the channel in **6** is estimated as the minimal distance between the closest non-bonded P atoms minus doubled van der Waals radius of P.¹³

¶ The outer diameter in **7** is calculated as the distance between the H atoms of two of the furthermost *Cp*⁺ ligands plus twice the van der Waals radii of H.¹³

|| The size of the void in **7** is calculated as the distance between the centroids of every individual *cyclo-P₄* unit and the centroid of the node minus twice the van der Waals radius of P (1.8 Å).¹³

- (a) F. J. Rizzuto, L. K. S. von Krbek and J. R. Nitschke, *Nat. Rev. Chem.*, 2019, **3**, 204; (b) Y. Sun, C. Chen and P. J. Stang, *Acc. Chem. Res.*, 2019, **52**, 802; (c) M. Fujita, M. Tominaga, A. Aoai and B. Therrien, *Acc. Chem. Res.*, 2005, **38**, 369; (d) M. Han, D. M. Engelhard and G. H. Clever, *Chem. Soc. Rev.*, 2014, **43**, 1848; (e) M. J. Wiester, P. A. Ulmann and C. A. Mirkin, *Angew. Chem., Int. Ed.*, 2011, **50**, 114; (f) J. Mendez-Arroyo, A. I. d'Aquino, A. B. Chinen, Y. D. Manraj and C. A. Mirkin, *J. Am. Chem. Soc.*, 2017, **139**, 1368; (g) H. Ruffin, S. A. Baudron, D. Salazar-Mendoza and M. W. Hosseini, *Chem.-Eur. J.*, 2014, **20**, 2449; (h) D. W. Agnew, I. M. DiMucci, A. Arroyave, M. Gembicky, C. E. Moore, S. N. MacMillan, A. L. Rheingold, K. M. Lancaster and J. S. Figueroa, *J. Am. Chem. Soc.*, 2017, **139**, 17257.
- (a) J. Bai, A. V. Virovets and M. Scheer, *Science*, 2003, **300**, 781; (b) M. Scheer, A. Schindler, C. Gröger, A. Virovets and



E. V. Peresypkina, *Angew. Chem., Int. Ed.*, 2009, **48**, 5046; (c) M. Scheer, A. Schindler, R. Merkle, B. P. Johnson, M. Linseis, R. Winter, C. E. Anson and A. V. Virovets, *J. Am. Chem. Soc.*, 2007, **129**(44), 13386; (d) H. Brake, E. Peresypkina, C. Heindl, A. V. Virovets and M. Scheer, *Chem. Sci.*, 2019, **10**, 29402.

3 E. V. Peresypkina, C. Heindl, A. Virovets, E. Mädl, H. Brake and M. Scheer, *Chem.-Eur. J.*, 2018, **24**, 2503; F. Dielmann, M. Fleischmann, C. Heindl, E. Peresypkina, A. V. Virovets, R. M. Gschwind and M. Scheer, *Chem.-Eur. J.*, 2015, **21**, 6208; C. Heindl, E. V. Peresypkina, A. V. Virovets, W. Kremer and M. Scheer, *J. Am. Chem. Soc.*, 2015, **137**, 10938; C. Schwarzmaier, A. Schindler, C. Heindl, S. Scheuermayer, E. Peresypkina, A. Virovets, M. Neumeier, R. Gschwind and M. Scheer, *Angew. Chem., Int. Ed.*, 2013, **52**, 10896; F. Dielmann, C. Heindl, F. Hastreiter, E. V. Peresypkina, A. V. Virovets, R. M. Gschwind and M. Scheer, *Angew. Chem., Int. Ed.*, 2014, **53**, 13605; C. Heindl, E. Peresypkina, A. V. Virovets, I. S. Bushmarinov, M. G. Medvedev, B. Krämer, B. Dittrich and M. Scheer, *Angew. Chem., Int. Ed.*, 2017, **56**, 13237.

4 E. Peresypkina, C. Heindl, A. Virovets and M. Scheer, Inorganic Superspheres, in *Clusters – Contemporary Insight in Structure and Bonding*, ed. S. Dehnen, 2016, vol. 174, pp. 321–373.

5 (a) O. J. Scherer, R. Winter and G. Wolmershäuser, *Z. Anorg. Chem.*, 1993, **619**, 827; (b) K. A. Mandla, M. L. Neville, C. E. Moore, A. L. Rheingold and J. S. Figueroa, *Angew. Chem., Int. Ed.*, 2019, **131**, 15473.

6 (a) B. P. Johnson, F. Dielmann, G. Balazs, M. Sierka and M. Scheer, *Angew. Chem., Int. Ed.*, 2006, **45**, 2473; (b) F. Dielmann, E. V. Peresypkina, B. Kraemer, F. Hastreiter, B. P. Johnson, M. Zabel, C. Heindl and M. Scheer, *Angew. Chem., Int. Ed.*, 2016, **55**, 14833.

7 M. Elsayed Moussa, M. Piesch, M. Fleischmann, A. Schreiner, M. Seidl and M. Scheer, *Dalton Trans.*, 2018, **47**, 16031; A. Cavaille, N. Saffon-Merceron, N. Nebra, M. Fustier-Boutignon and N. Mezailles, *Angew. Chem., Int. Ed.*, 2018, **57**, 1874.

8 (a) S. Deng, C. Schwarzmaier, M. Zabel, J. F. Nixon, M. Bodensteiner, E. V. Peresypkina, G. Balazs and M. Scheer, *Eur. J. Inorg. Chem.*, 2011, **2011**, 2991; (b) M. Elsayed Moussa, M. Seidl, G. Balazs, M. Zabel, A. V. Virovets, B. Attenberger, A. Schreiner and M. Scheer, *Chem.-Eur. J.*, 2017, **23**, 16199.

9 (a) V. A. Blatov, A. P. Shevchenko and D. M. Proserpio, *Cryst. Growth Des.*, 2014, **14**, 3576; (b) V. A. Blatov, M. O'Keeffe and D. M. Proserpio, *CrystEngComm*, 2010, **12**, 44; (c) M. O'Keeffe, M. A. Peskov, S. J. Ramsden and O. M. Yaghi, *Acc. Chem. Res.*, 2008, **41**, 1782.

10 (a) T. C. Stamatatos, S. Mukherjee, K. A. Abboud and G. Christou, *Chem. Commun.*, 2009, 62; (b) F. Xu, H. N. Miras, R. A. Scullion, D.-L. Long, J. Thiel and L. Cronin, *Proc. Natl. Acad. Sci. U. S. A.*, 2012, **109**, 11609; (c) J.-D. Leng, J.-L. Liu and M.-L. Tong, *Chem. Commun.*, 2012, **48**, 5286; (d) P. Klufers and J. Schuhmacher, *Angew. Chem., Int. Ed.*, 1994, **33**, 1863.

11 C. Zhao, Y.-Z. Han, S. Dai, X. Chen, J. Yan, W. Zhang, H. Su, S. Lin, Z. Tang, B. K. Teo and N. Zheng, *Angew. Chem., Int. Ed.*, 2017, **56**, 16252.

12 *CHEM3D Ultra* by Perkin Elmer, 2017, version 17.0.0.206.

13 M. Mantina, A. C. Chamberlin, R. Valero, C. J. Cramer and D. G. Truhlar, *J. Phys. Chem. A*, 2009, **113**, 5806.

